Optical and structural properties of organic-inorganic hybrid perovskite(C12H25NH3)2PbI4multiple quantum well embedded in porous anodic alumina

W. Zaghdoudi [1*], A. Bardaoui[1], Y. Abid[2], H. Elhouichet[3] and R. Chtourou[1]

[1]*Laboratoire de Photovoltaique Centre de Rechercheet des Technologies de l'Energie,*

[2]*Laboratoire de Physique Appliquee, Faculte des sciences de Sfax, BP802, Sfax 3018,Tunisia*

[3]*Laboratoire des MateriauxMinerauxetLeurs Applications, Centre National de Recherches en Sciences des Materiaux, B.P. 95, Hammam-Lif 2050, Tunisia*

Email: walid_inrst@yahoo.fr

Abstract: In the present work, organic-inorganic hybrid perovskite (C12H25NH3)2PbI4multiple quantum well (C12PbI4 QW) embedded in porous anodic alumina (PAA) thin films on glass and aluminum substrates are investigated in detail. The porosity and the uniformly arranged structure of these films are examined using Scanning Electron Microscopy (SEM).

The use of two different substrates enables the PAA templates obtained by anodization in an acid electrolyte solution to have different pore dimensions. The synthesized films are characterized morphologically using the atomic force microscopy (AFM). The crystallographic structure is examined by means of X-ray diffraction (XRD). Finally, the optical characterizations are studied using a UV-Vis-NIR spectrometer and photoluminescence (PL) measurements. The effect of the two different substrates on the impregnation of the C12PbI4 QW in the PAA is presented. Both PL and AFM studies show a better penetration of the C12PbI4 QW in the case of the Al substrate providing a wider pore diameter. It results in a better quantum confinement leading to a PL blue shift more pronounced when the C12PbI4 QW are embedded into the pores of the PAA on Al substrate.

Keyword: Porous anodic alumina; Perovskites; AFM microscopy; XRD; Photoluminescence; UV-Vis spectroscopy.

1. Introduction:

Hybrid organic-inorganic perovskite semiconductors have been the subject of intensive research thanks to their unique flexibility in structure and their remarkable electroopticalproperties. These hybrids form natural multiple quantum well (QW) structures, where wells of the 2D inorganic layer are sandwiched between barriers of the organic layers. It results in a quantum confinement as well as in a dielectric confinement of the carriers within the inorganic layers, and thus the formation of stable excitons with large binding energies even at room temperature. Such structures exhibit in fact strong excitonic absorption and emission features of great interest for optoelectronic

applications such as light emitting diodes, organic-inorganic field effect transistors, and optical switches based on strong exciton-photon coupling in microcavity photonic architectures [1,2].

Due to the continual demand for reduction in device size and because of the methodology limitation to obtain uniform and highly ordered thin films based on these QW hybrids, a great idea consists in synthesizing the desired material within the pores of a nanoporous membrane [3]. One of the attractive templates is porous anodic alumina (PAA).

The PAA membrane have indeed received much attention because of the new perspectives it offers in electronic, photovoltaic, and optoelectronic nanodevices applications [4,5] and also as a template for fabricating various nanostructured materials such as carbon and Ni nanotubes, Si nanodots, CdS nanoparticles and ZnO nanowire arrays [6-7].

Under proper conditions the pores order themselves into a very regular vertical pores of controlled sizes. The ordering has been attributed to the reaction of the mechanical stress that exists upon the conversion of aluminum to aluminum oxide and the subsequent volume expansion. The geometry of the PAA is characterized by a close-packed array of columnar hexagonal cells, each containing a central pore [8]. The formed pores have been found to be uniform and nearly parallel, making the PAA film an ideal template for deposition.

In this work, we report the synthesis of hybrid organic-inorganic perovskite (C12H25NH3)2PbI4QW (abbreviated C12PbI4 QW), deposited on a PAA membrane with different pore diameters. The morphology of the synthesized structures were studied using Scanning Electron Microscopy (SEM), the microstructural properties were analyzed by X-ray Diffraction (XRD) and finally, the optical characterizations were investigated by means of photoluminescence (PL) and UV-Vis spectroscopies.

2. Experimental

Porous anodic alumina, with different pore diameters, ranging from 10 to 50 nm, was fabricated first using aluminum substrates and second using evaporated aluminum on glass substrates. The glass substrate was coated with a thin aluminum layer of 0.5 μm thickness using the evaporation technique and a mirror-like aluminum layer is obtained. The aluminum is then cut into pieces to obtain several samples of 25×25 mm. These samples were then inserted into the anodization jacket. The anodic alumina template is fabricated by anodizing aluminum in an acid electrolyte solution. The anodization was carried out potentiostatically ina 10% sulfuric acid solution [9, 10]. Aluminum foil is used as the anode and a Platinum mesh as the cathode. A DC voltage of 15 V and of 40 V is then applied across the two electrodes respectively for the evaporated aluminum on glass substrates and for the aluminum substrates, at a temperature of 288 K. During the process, a layer of aluminum oxide is formed and is simultaneously locally dissolved by hydrogen ions, assisted by the applied electric field.
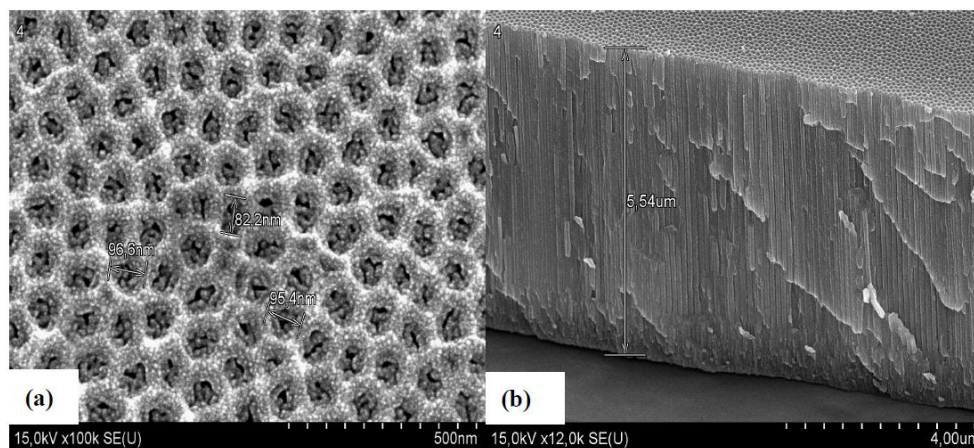
Fig.1: SEM images of a PAA template: (a) the top view and (b) the cross-sectional view.

Figure 1 shows the SEM image of an example of PAA. We remark that the pores with a relative uniform size are hexagonally arranged with a high regularity. The mean diameter of the holes, as measured from the SEM images, was about 50 nm. The cross-sectional view shows that the holes were non-intercepting and parallel cylinders. The thickness of the template is about 5.54 µm.

For the $(C_{12}H_{25}NH_3)_2PbI_4$ synthesis, the first step consist of preparing the iodine salts $C_{12}H_{25}NH_3I$ by treating butylamine $(C_{12}H_{25}NH_2)$ with hydroiodic acid (HI) (aqueous solution, 57%) at room temperature. The next step consists of mixing Stoichiometric amounts of $(C_{12}H_{25}NH_3$ I) and PbI_2 in N,N-dimethylformamide as a common solvent. The resulting solution is then kept at room temperature. After two weeks of evaporation, we have obtained platelets crystals. The purity of the solution was improved by second recrystallization. Schematic structure of layered perovskite compound $(C_{12}H_{25}NH_3)_2PbI_4$ is presented in figure 2. The $C_{12}PbI_4$ QW was then deposited onto PAA with variable thickness and pores diameters. For comparison purposes, we have also prepared $C_{12}PbI_4$ QW on glass substrate. The synthesized films were characterized morphologically using the atomic force microscope (AFM) from Veeco Instruments. The crystallographic structure was examined by means of X-ray diffraction (XRD) using a Philips X'pert-MPD x-ray diffractometer (Co Kαradiation) in 2θ interval ranging from 10◦ to 80◦. Reflectivity spectra were recorded using the LAMBDA 950 UV/Vis/NIR Perkin Elmer spectrometer. Photoluminescence measurements were performed using a variable temperature (10K–300K) close-cycle cryostat under 458 nmline of an Argon ion Ar+ laser as excitation source. The excitation wavelengths were selected to show the maximum photoluminescence intensity. The signal was detected through a 250 mm Jobin-Yvonmonochromator and by a GaAsphotomultiplier associated with a standard lock-in technique.
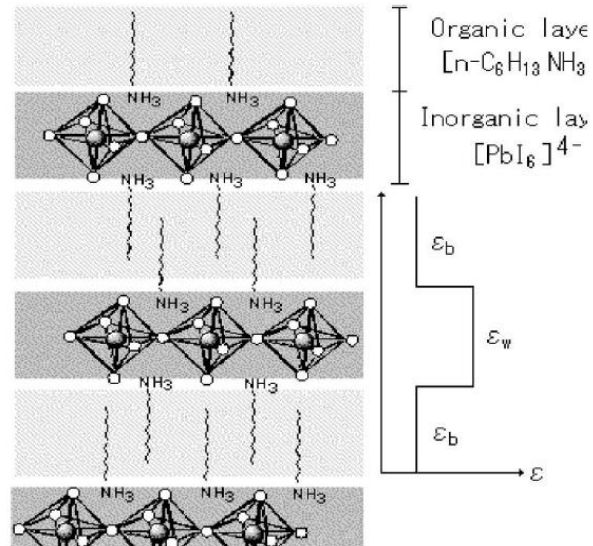
Fig.2: Schematic structure of layered perovskite compound (C$_{12}$H$_{25}$NH$_3$)$_2$PbI$_4$.ε$_w$ and ε$_b$ are the dielectric constants of the inorganic and organic layers respectively.

3. Results and discussion

3.1 Morphological characterization

Figure 3 shows the 2D and 3D AFM images of a PAA/Glass before and after the impregnation of the perovskite C$_{12}$PbI$_4$ QW. The ordered pore arrays had a pore diameter of about 10 nm and a thickness of about 0.5 μm, with a smooth and clean surface area surrounding the pores.
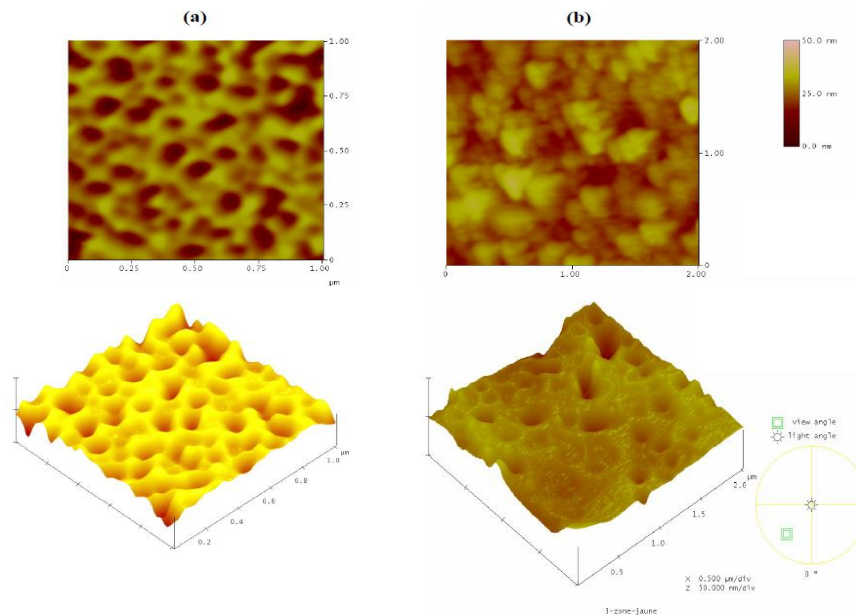

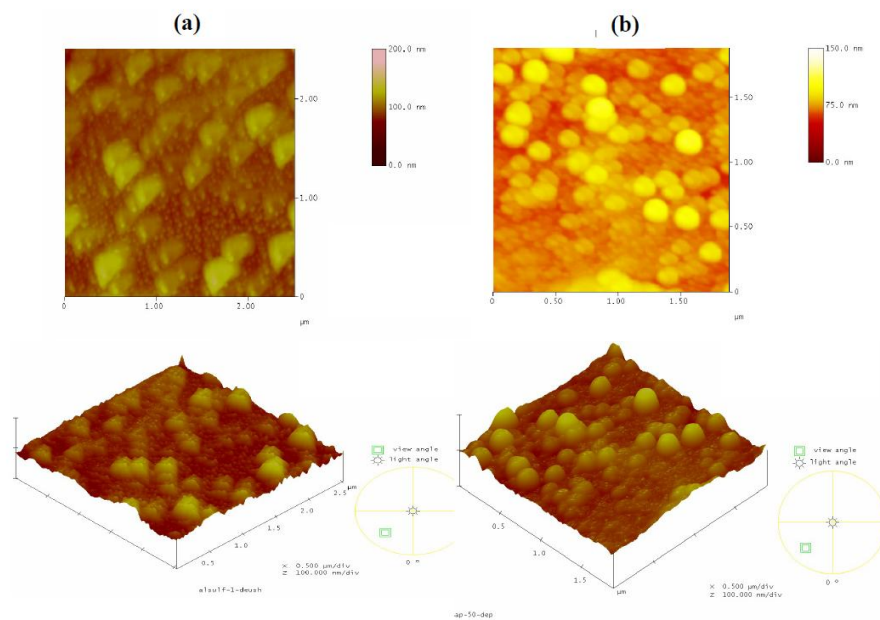**Fig.3:** 2D and 3D AFM images of a PAA/Glass with 10 nm pore diameter. (a) before and (b) after the impregnation of the perovskite C$_{12}$PbI$_4$ QW.

Fig.4: 2D and 3D AFM images of a PAA/Al with 50 nm pore diameter. (a) before and (b) after the impregnation of the perovskite C$_{12}$PbI$_4$ QW.

In figure 4, 2D and 3D AFM images of a PAA/Al before and after the impregnation of the perovskite C12PbI4 QW. The surface shows spherical domes with an average size varying approximately from 35 to 50 nm. The thickness was estimated to be 5.54 μm thicknesses. For both substrates, the surface morphology was obviously changed after the C12PbI4 overlaid on the original smooth surface inside surrounding the pores.

We notice that the use of the Al substrate enabled a better impregnation of the C12PbI4 QW thanks to the wider pore diameter of the PAA template. This led to the formation of autoorganizedislets and thus to a better confinements of the perovskite QW.

The WSxM5.0 software was used to obtain the particle height distribution calculated from the roughness histogram as shown in figure 5. The maximal height (topography) of the superficial grains for the samples C12PbI4/PAA/Glass and C12PbI4/PAA/Al is 47.5 and 82.9 nm, respectively. The number of grains in depth of the porous region is important and differs from a sample to another. For the samples C12PbI4 /PAA/Glass and C12PbI4/PAA/Al, the maximum number of grains is estimated to be, in the 5 μm2 area of the samples, 13386 and 12109 attributable to a particles height about 14.8 and 21.7 nm, respectively (figure 5).
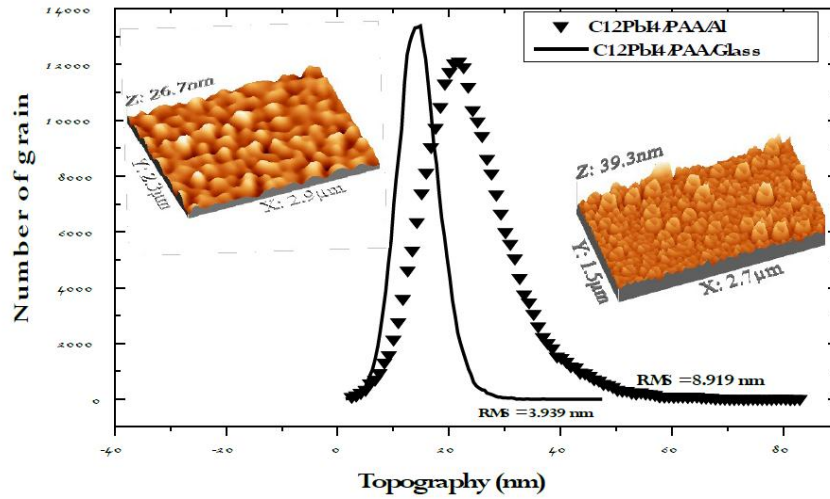
Fig.5: Roughness histograms of the C12PbI4 QW embedded on different porous anodic alumina substrates.

3.2 Microstructural characterization

Figure 6 gives the X-ray diffractogram of the C12PbI4/PAA grown directly on a glass substrate. The XRD spectra reveal the crystal structure of the C12PbI4/PAA/Glass. All specimens gave similar XRD patterns, indicating the high crystallinity of C12PbI4 films deposited on porous alumina. The C12PbI4 crystals have indeed been self-organised into the porous anodic alumina films.
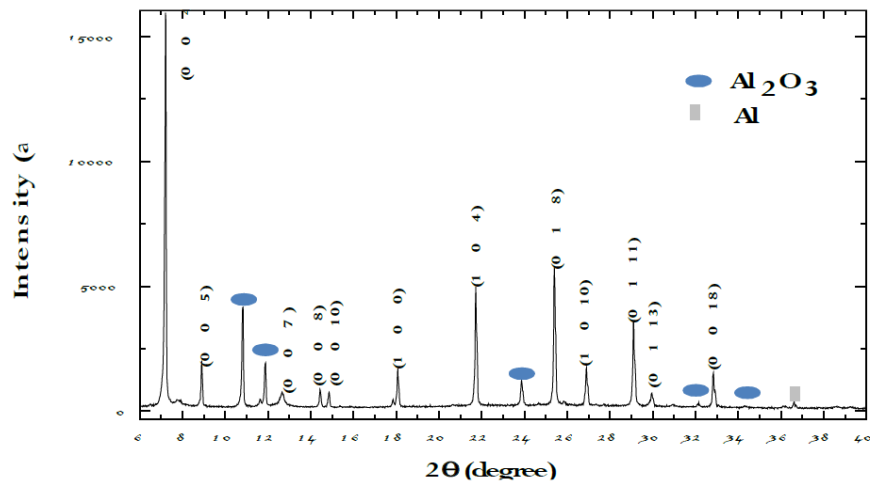

Fig.6: X-ray diffraction patterns of C12PbI4 QW deposited on porous alumina films. (Co Kα (λ = 1.8997 A°)).

3.3 Optical characterization

$C_{12}PbI_4$ deposited on PAA gave an interesting PL response, large bending energy and a good confinement effect, contrarily to previous works where C12PbI4 are formed on TiO2 thin films; the PL was almost totally quenched [11].

It has been reported that binding energy of an exciton in the inorganic layer of material exhibiting a multi quantum well structure is enhanced not only by the low dimensionality but also by large difference in the dielectric constants between the layers. In $C_{12}PbI_4$ the dielectric constants of the inorganic and organic layers are $\varepsilon w = 6.1$ and $\varepsilon b = 2.1$, respectively [12]. The binding energy of excitons in C12PbI4 has been estimated to be several hundred meV, which leads to a strong photoluminescence (PL) of this material even at room temperature (RT) [13].

Figure 7 shows the PL spectra, recorded at room temperature, of the organic-inorganic perovskite $C_{12}PbI_4$ and the PAA templates before and after the insertion of the $C_{12}PbI_4$, for both substrates (i.e. glass and Al). These spectra were taken after the rinsing procedure.
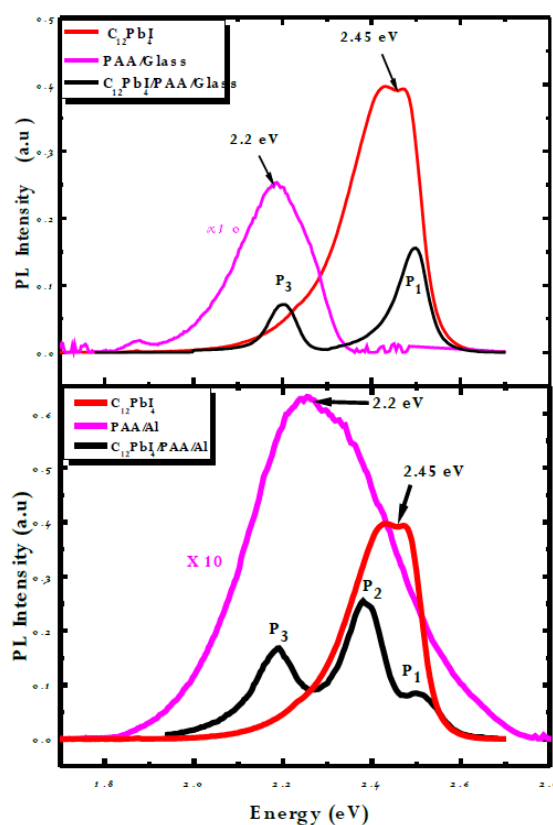

Fig.7: Room temperature PL spectra of (a) the reference sample C12PbI4, PAA/Glass and C12PbI4 /PAA/Glass and (b) the reference sample C12PbI4, PAA/Al and C12PbI4 /PAA/Al.

The $C_{12}PbI_4$ reveals a PL band at 2.45 identified as an excitonic emission peak which may be due to the transfer of energy between the carbon and iodide (II).

The PAA templates grown on both substrates exhibits a relatively low PL band situatedapproximately at 2.2 eV, wider and slightly more intense in the case of the Al substrate having the largest pores. Thus, this PL enhancement is due to pore size which has a significant effect. In fact, the PL increases with increasing the pore size of the PAA membranes. This PL response is attributed to the presence of singly ionized oxygen vacancies

(F+ centers) [14].

After the deposition of the C12PbI4 QW, we notice two different behaviors depending on the pores size. In the case of the glass substrate, we notice the presence of two peaks P1 and P3 situated at 2.5 and 2.2 eV respectively. On the other hand, in the case of the Al substrate, besides the peaks P1 and P3 located respectively at 2.51 and 2.2 eV. We notice the appearance of a new peak noted P2 at 2.38 eV.

The peak P3 obviously originated from the PAA since it doesn't exist in the PL response of the perovskite $C_{12}PbI_4$ QW alone, while the peaks P1 and P2 seem to have their origin from the C12PbI4 QW embedded in the PAA matrix. To better understand the behavior of the $C_{12}PbI_4$ QW incorporation into the PAA for both substrates, we propose a correlation between PL and UV-Vis absorption measurements, as shown in figure 8. We notice from figure 8a, a clear blue shift of the peak P1 when the $C_{12}PbI_4$ QW is deposited on top of the PAA in comparison to the PL response of the $C_{12}PbI_4$ QW alone. This blue shift is more pronounced in the case of the Al substrate which confirms, as in the AFM study, that the $C_{12}PbI_4$ QW was better confined in the case of the wider pores.
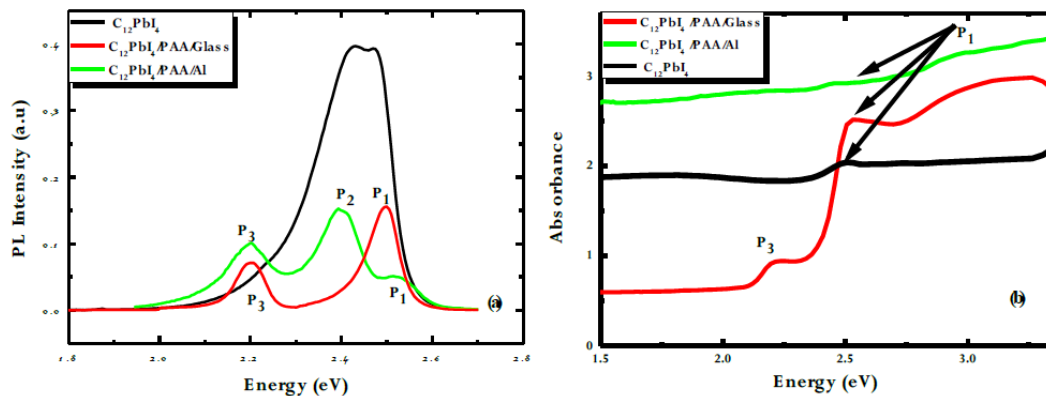

Fig.8: Room temperature PL spectra of (a) the reference sample C12PbI4, PAA/Glass and C12PbI4 /PAA/Glass and (b) the reference sample C12PbI4, PAA/Al and C12PbI4 /PAA/Al.

From the absorption spectra presented in figure 8a, we also notice the same behavior of the absorption peak P1 attributed to the excitonic band localized in the inorganic part of the hybrid material and which was shifted from the band of the $C_{12}PbI_4$ QW alone.

The observed blue shift of both PL and absorption measurements is indeed the result of the quantum confinement of electrons and holes in $C_{12}PbI_4$ QW embedded in the PAA matrix. In fact, quantum confinement of charge carriers in small pores leads to new effects in the optical properties, such as the blue shift of exciton spectral lines originating

from the increase of the kinetic energy of the charge carriers and the increase of the oscillator strength per volume unit [15, 16]. These effects are quite important when the size of the particles is at the nanometer scale, which is the case of the used PAA templates considered as good matrices, for the incorporation of such QW structures, in order to realize the confinement regime for charge carriers.

Figure 9 shows a correlation of room temperature reflectivity and PL spectra of $C_{12}PbI_4$ deposited on PAA for both glass and aluminum substrates having pore diameters around 10 and 50 nm respectively. We notice the presence of two absorption bands assigned to free excitons and to unbounded electron–hole pair transitions and located at 2.48 and 2.55 eV, respectively for the glass and the Al substrates. These bands corresponds to the PL peak P1 with a shift that increases from 5 to 80 meV as the pore diameters increase from to 10 to 50 nm. This is the stocks shift which is due to the vibrational relaxation of the exited $C_{12}PbI_4$ on PAA to the ground state [17].
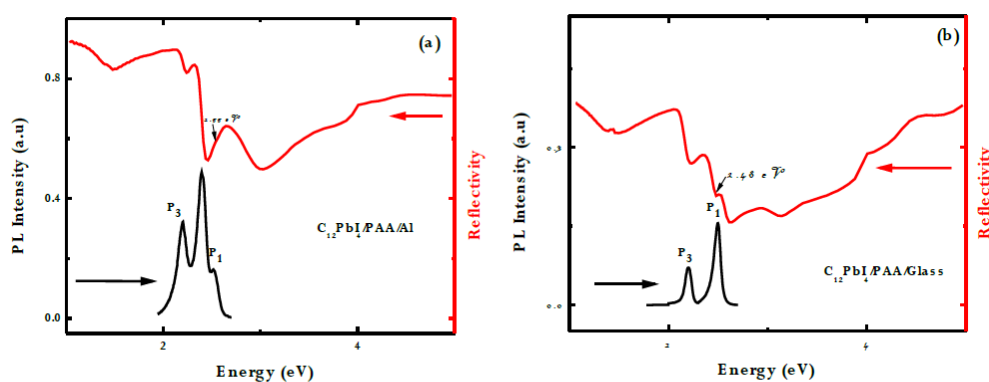

Fig.9: Room temperature PL and reflectivity spectra of $C_{12}PbI_4$ incorporated in PAA formed (a) on an Al substrate and (b) on a Glass substrate.

The reflectivity spectra of the pure and $C_{12}PbI_4$ deposited on PAA templates on an Al substrate are shown in figure 10 (red dashed line). The upper line (black line) represents the small difference between the peak and the valley, meaning that no effective interference was established in the pure PAA template. We note this difference is enhancement from 18.36% to 42.75%. This is due to the the increase of the absorption after the deposition the $C_{12}PbI_4$ and which confirms the strong confinement shown in the last study.
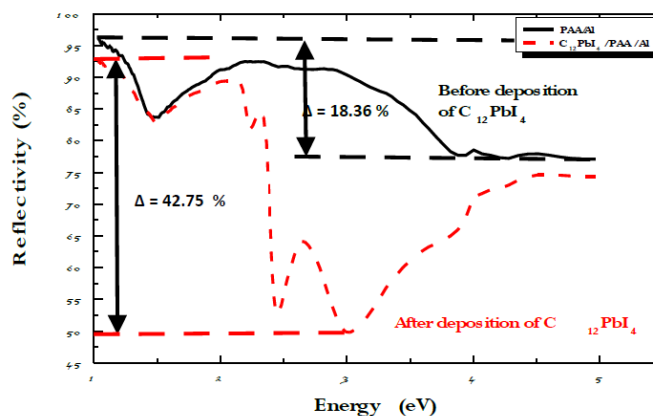

Fig.10: Reflectivity spectra of PAA template with 50 nmpore diameter before and after the impregnation of the perovskite C12PbI4 QW.

Conclusions

A simple approach of fabricating high-quality and highly luminescent hybrid inorganicorganicQW structures embedded in porous anodic alumina was presented. Organic-inorganic perovskite $C_{12}PbI_4$ QW embedded in porous anodic alumina (PAA) thin films on glass andaluminum substrates were investigated in detail. Morphological study of the synthesized films was performed using AFM, microstructural properties were examined by means of XRD and optical characterizations were studied using a UV-Vis-NIR spectrometer and PL measurements. The use of two different substrates had an important effect on the impregnation of the $C_{12}PbI_4$ QW in the PAA. A better penetration of the $C_{12}PbI_4$ QW in the case of the Al substrate providing a wider pore diameter was demonstrated and a better quantum confinement was observed resulting in a PL blue shift more pronounced when the $C_{12}PbI_4$ QW are embedded into the pores of the PAA on Al substrate.

References

[1] M. Era, S. Morimoto, T. Tsutsui, and S. Saito, Appl. Phys. Lett. 65, 676 (1994).

[2] K. Sumioka, H. Nagahama, and T. Tsutsui, Appl. Phys. Lett. 78, 1328 (2001).

[3] Martin CR, Chem Mater 8, 1739 (1996).

[4] R.E.Ricker, A.E.Miller, D.F.Yue, and G.Ganejee, J. Electron. Mater. 25, 1585 (1996).

[5] M.Sun, G.Zangari, M.Shamsuzzoha and R.M.Metzger, Appl. Phys. Lett. 78, 2964 (2001).

[6] Keller F, Hunter M S and Robinson D L 1953 J. Electrochem. Soc. 100 411.

[7] Hoyer P, Baba N and Masuda H 1995 Appl. Phys. Lett. 66 (2700).

[8] H.Masuda and K.Fukuda, Science, 268, 1466 (1995).

[9] G.D. Sulka, M. Jaskuła, J. Nanosci. Nanotechnol. 6 (2006) 3803.

[10] G.D. Sulka, V. Moshchalkov, G. Borghs, J.-P. Celis, J. Appl. Electrochem. 37 (2007) 789.

[11] C.R. Li, H.T. Deng, J. Wan, Y.Y. Zheng, and W.J. Dong, Materials Letters 64 (2010) 2735–2737.

[12] K. Shibuya et al. / Nucl. Instr. and Meth. In Phys. Res. B194 (2002) 207–212.

[13] Kenichiro Tanaka, Takashi Kondo, Science and Technology of Advanced Materials 4 (2003)599–604.

[14] G.S. Huang, X.L. Wu, Y.F. Mei, X.F. Shao, J. Appl. Phys. 93 (2003) 582.

[15] L. E. Brus, J. Phys. Chem. 90 (1986) 2555.

[16] B.O. Dabbousi, J. Rodriguez-Viejo, F.V. Mikulec, J.R. Heine, H. Mattoussi, R. Ober, K.F. Jensen and M.G. Bawendi, J. Phys. Chem. B 101 (1997) 9463.

[17] Franceschetti and S. T. Pantelides, Phys. Rev. B 68 (2003) 033313.